One Health 22 (2026) 101409

Contents lists available at ScienceDirect

One Health

journal homepage: www.elsevier.com/locate/onehlt

Genomic characterization and global lineage–plasmid context of a *bla*$_{NDM-5}$-harboring *Escherichia coli* ST3014 isolate

Zheng-Ze He [a,1], Chao Lv [a,b,c,1], Feng Xie [b], Kun Wang [d], Qing-Qing Zhang [e], Wei-Ye Chen [c], Ya-Qi He [a], Yang Hong [a,b], Jing Xu [a,b,c,*], Xiao-Nong Zhou [a,b,c,*]

[a] National Institute of Parasitic Diseases, Chinese Center for Disease Control and Prevention (Chinese Center for Tropical Diseases Research), National Health Commission Key Laboratory of Parasite and Vector Biology, WHO Collaborating Centre for Tropical Diseases, National Center for International Research on Tropical Diseases, Shanghai, China
[b] Hainan Center for Tropical Diseases Research (Hainan Sub-Center of Chinese Center for Tropical Diseases Research), Haikou 571199, Hainan, China
[c] School of Global Health, Chinese Center for Tropical Diseases Research, Shanghai Jiao Tong University School of Medicine, Shanghai, China
[d] School of Public Health, Hangzhou Medical College, Hangzhou 310013, China
[e] The Sanya Institute of Nanjing Agricultural University, Laboratory of Emerging Animal Diseases and One Health, Nanjing Agricultural University, Nanjing 210095, China

ARTICLE INFO

Keywords:
Escherichia coli
ST3014
bla$_{NDM-5}$
IncF plasmid
One health

ABSTRACT

Background: The global emergence and dissemination of carbapenem-resistant Enterobacterales pose a substantial public-health threat. However, *Escherichia coli* (*E. coli*) sequence type 3014 (ST3014), including *bla*$_{NDM}$-positive representatives, remains poorly characterized across human, animal, and environmental interfaces. Here, we characterized the genomic features of a *bla*$_{NDM-5}$-harboring ST3014 isolate and its associated plasmid background to provide a lineage- and plasmid-focused framework for future surveillance.

Methods: Two *bla*$_{NDM}$-positive *E. coli* isolates (E44 and E56) were recovered from 60 piglet fecal samples collected from an intensive swine farm in Qionghai City, Hainan Province. Whole-genome sequencing identified E44 as a *bla*$_{NDM-5}$-positive ST3014 isolate and E56 as a *bla*$_{NDM-1}$-positive ST9547 isolate. Because *bla*$_{NDM-5}$ differs from *bla*$_{NDM-1}$ by amino acid substitutions associated with enhanced carbapenem hydrolytic activity and broader dissemination potential, subsequent genomic characterization focused on the *bla*$_{NDM-5}$-positive isolate E44. The selected isolate underwent short- and long-read sequencing, followed by hybrid assembly and functional annotation. To contextualize its genomic characteristics, a global *E. coli* ST3014 dataset was compiled from EnteroBase, NCBI, and published literature to assess antimicrobial resistance genes (ARGs), virulence factors (VFs), and core-genome phylogeny. Furthermore, the *bla*$_{NDM-5}$-carrying plasmid from E44 was queried against the PIPDB database, plasmid-level phylogenetic relatedness was inferred using Mash distances, and the *bla*$_{NDM-5}$ genetic context of E44 was compared with those of other *bla*$_{NDM-5}$-carrying plasmids.

Results: The *bla*$_{NDM-5}$-positive ST3014 isolate E44 carried 6 ARGs and 42 VFs, with *bla*$_{NDM-5}$ located on a 124-kb IncF multireplicon plasmid. In addition to multiple resistance determinants, this plasmid co-harbored ExPEC-associated siderophore/iron-uptake loci, including *sitABCD* and *iucABCD-iutA*. A global dataset comprising 82 ST3014 *E. coli* isolates demonstrated broad geographic and ecological dissemination across 23 countries, spanning human, animal, and environmental sources. A time-scaled phylogeographic reconstruction suggested that ST3014 most likely originated in Asia, with China showing the highest country-level likelihood, and indicated repeated international dissemination after 2010. Phylogenetic analysis of 153 homologous plasmids showed that related IncF plasmids are distributed across diverse Enterobacterales hosts, with *E. coli* as the predominant host; notably, the *bla*$_{NDM-5}$-harboring plasmid identified in E44 (designated E44-plasmid1) was most closely related to an *E. coli*-derived plasmid. Comparative analysis of *bla*$_{NDM-5}$ genetic contexts revealed a conserved *bla*$_{NDM-5}$-associated core module (*ble-trpF-dsbD*) embedded in variable flanking regions, with recurrent *IS26* adjacent to the upstream segment, consistent with local recombination and modular remodeling around the resistance locus.

* Corresponding author at: National Institute of Parasitic Diseases, Chinese Center for Disease Control and Prevention (Chinese Center for Tropical Diseases Research), National Health Commission Key Laboratory of Parasite and Vector Biology, WHO Collaborating Centre for Tropical Diseases, National Center for International Research on Tropical Diseases, Shanghai, China.
E-mail addresses: xujing@nipd.chinacdc.cn (J. Xu), zhouxn1@chinacdc.cn (X.-N. Zhou).
[1] These authors contributed equally to this work.

https://doi.org/10.1016/j.onehlt.2026.101409
Received 22 January 2026; Received in revised form 1 April 2026; Accepted 7 April 2026
Available online 9 April 2026

Conclusions: The detection of a *bla*$_{NDM-5}$-harboring ST3014 isolate in a breeding-farm setting, together with the broad distribution of related strains and plasmids in public datasets, suggests a potential One Health concern warranting continued surveillance.

1. Introduction

Antimicrobial resistance (AMR) has become a pressing global concern, exerting significant impacts on public health, economic stability, and food security [1]. The worldwide emergence of carbapenem-resistant Enterobacteriaceae (CRE) has steadily compromised the clinical effectiveness of carbapenems, which are regarded as the last-resort antibiotics against infections caused by multidrug-resistant (MDR) Gram-negative pathogens [2]. Carbapenemases can hydrolyze nearly all β-lactam antibiotics, rendering almost all agents in this class ineffective [3]. Importantly, carbapenem resistance determinants are frequently located on conjugative plasmids, and their horizontal transmission among diverse strains and species has markedly accelerated the global dissemination of these resistance traits [4]. In the 2024 WHO bacterial priority pathogens list, carbapenem-resistant *Escherichia coli* was recognized as a critical-priority pathogen [5]. Global genomic surveillance has further shown that carbapenem-resistant *E. coli* (CREC) is widely distributed across countries and often exhibits frequent plasmid-mediated transmission events, highlighting the need to understand resistance dissemination at both the clonal and plasmid levels [6,7]. The global spread of New Delhi metallo-β-lactamases (NDM) has transformed carbapenem resistance into a major clinical threat.

Carbapenemase-encoding resistance genes comprise a diverse array of variants, including *bla*$_{NDM}$, *bla*$_{VIM}$, *bla*$_{IMP}$, *bla*$_{KPC}$, and OXA-48-like family [8]. Among the various carbapenem resistance genes, *bla*$_{NDM}$ poses a particular threat owing to its exceptional capacity for dissemination [9]. Since the first identification of *bla*$_{NDM-1}$ in *Klebsiella pneumoniae* in 2008 [10], multiple variants have been reported worldwide, and predominantly identified among members of the Enterobacterales [3]. These genes, especially *bla*$_{NDM-5}$, were frequently located on conjugative plasmids such as IncX3, which substantially facilitate their rapid spread and make them key drivers of the current global CRE burden [11]. Beyond dissemination of the resistance determinant itself, plasmid backbones carrying *bla*$_{NDM}$ may also accumulate additional antimicrobial resistance genes (ARGs), insertion sequences, and, in some cases, virulence-associated loci, thereby promoting persistence and cross-host adaptation. Comparative analyses have shown that *bla*$_{NDM}$-bearing plasmids circulate across diverse Enterobacterales hosts and that the surrounding mobile genetic elements [12], particularly *IS26* and related insertion sequences [13], play a major role in the assembly and remodeling of *bla*$_{NDM}$ genetic contexts. Therefore, characterization of both the bacterial host lineage and the *bla*$_{NDM}$-carrying plasmid is essential for understanding the dissemination potential of carbapenem resistance [12].

The extensive and often inappropriate use of antibiotics in intensive livestock production has promoted colonization of resistant bacteria in the animal gut, making food animals important reservoirs of ARGs [14]. Although carbapenems are strictly reserved for human clinical use and are not approved for routine application in food animals [15], increasing evidence has documented the emergence of carbapenem resistance in food animals worldwide. Among these genes, *bla*$_{NDM-5}$ has been reported repeatedly as a prominent variant in animal and food associated isolates [16]. In China, *bla*$_{NDM-5}$ has been reported in isolates from poultry farms, retail eggs and other food-related matrices, indicating that food animals and associated environments may act as reservoirs and potential sources for transmission of clinically relevant ARGs to humans through direct contact, environmental contamination, and the food chain [17].

In contrast to globally dominant high-risk *E. coli* lineages such as ST131, ST167, or ST410, ST3014 has received little dedicated attention in the literature. Available reports suggest that this sequence type has been detected only sporadically across different ecological interfaces, including human clinical isolates [18], farming soil [19], and food-related samples [20], indicating that it is not restricted to a single host or setting. Notably, *bla*$_{NDM-5}$-positive ST3014 has already been identified in retail egg-associated *E. coli*, suggesting that this lineage is capable of acquiring clinically important carbapenem-resistance determinants in the food chain [20]. However, to our knowledge, no lineage-focused study has systematically characterized the global distribution, resistome/virulome features, phylogenetic relationships, and homologous *bla*$_{NDM}$-carrying plasmid background of *E. coli* ST3014. This knowledge gap makes a global genomic investigation of *bla*$_{NDM-5}$-positive ST3014 both timely and necessary.

Hainan Province is an important livestock-producing region in tropical China. However, publicly available molecular epidemiological studies specifically focusing on *bla*$_{NDM}$-positive *E. coli* from food-animal settings in Hainan remain limited [21,22], especially when viewed against the growing number of related reports from eastern coastal China [17]. This regional data gap highlights the need for genomic investigation of locally circulating resistant isolates and their associated mobile genetic elements.

Recently, a *bla*$_{NDM-5}$-harboring *E. coli* isolate recovered from piglet feces in Qionghai City, Hainan Province, was identified as ST3014. In this study, we performed short- and long-read whole-genome sequencing to characterize the genomic features of this isolate and its *bla*$_{NDM-5}$-carrying plasmid, and then placed it within a global ST3014 genomic framework compiled from public databases and published literature. By integrating lineage-level and plasmid-level analyses, this study aimed to clarify the genomic characteristics, evolutionary context, and dissemination potential of *bla*$_{NDM-5}$-positive *E. coli* ST3014.

2. Materials and methods

2.1. Sample collection and bacterial isolation

A total of 60 rectal swab samples were collected from piglets at a swine farm in Qionghai City, Hainan Province. Each rectal swab was placed into 5 mL of Luria Bertani (LB) broth and incubated at 37 °C with shaking at 180 rpm for 4–6 h for pre-enrichment. Subsequently, 50 μL of the enrichment culture was inoculated into 1.5 mL of LB broth supplemented with the meropenem (2 μg/mL) and incubated at 37 °C for 18–24 h for preliminary screening. Cultures that remained clear were discarded, whereas those exhibiting turbidity were streaked onto MacConkey agar plates containing meropenem (2 μg/mL) and incubated at 37 °C for another 18–24 h. After primary screening on meropenem-containing MacConkey agar, one suspected colony was selected from most positive samples, whereas two morphologically distinct suspected colonies were selected when more than one colony type was observed. In total, 72 suspected colonies were collected for secondary screening.

Species identification was performed by PCR amplification using primers targeting a 272-bp fragment (forward: GCCTCGCCTGGAGAATGA; reverse: CCTGAGACTGCGGTGGAA) [23]. Screening for the carbapenemase gene *bla*$_{NDM}$ was conducted using primers amplifying a 217-bp fragment (forward: CAGTCGCTTCCAACGGTTTG; reverse: AACGCATTGGCATAAGTCGC) [24]. PCR reactions were performed in a 20 μL system consisting of 10 μL of 2× PCR Master Mix, 1 μL of each primer, 2 μL of DNA template, and 6 μL of nuclease-free water. The thermal cycling protocol was as follows: an initial denaturation at 94 °C for 5 min; 35 cycles of denaturation at 94 °C for 30 s, annealing at 55 °C for 30 s, and extension at 72 °C for 30 s; followed by a final extension at 72 °C for 10 min. PCR products were then held at 4 °C until further

analysis.

Based on the above procedures, 44 isolates were confirmed as *E. coli*, among which two isolates were positive for bla_{NDM} by PCR. These two isolates were designated E44 and E56 and were both subjected to whole-genome sequencing for sequence typing and bla_{NDM} variant determination. Because only E44 was identified as bla_{NDM-5}-positive ST3014, subsequent lineage-focused comparative analyses were performed on E44.

2.2. Whole-genome sequencing, assembly, annotation and typing

Genomic DNA was extracted from the *E. coli* isolate using a commercial bacterial DNA extraction kit (Personalbio, Shanghai, China) according to the manufacturer's instructions. Sequencing libraries were constructed following the standard protocols for both Illumina and Oxford Nanopore platforms using commercial library kits (Personalbio, Shanghai, China).

Short-read sequencing was performed on the Illumina NovaSeq 6000 platform, generating 150-bp paired-end reads with an average coverage depth exceeding 100×. Long-read sequencing was conducted using the Oxford Nanopore PromethION platform, generating reads with an average coverage depth exceeding 50×. A hybrid genome assembly strategy was employed: long- and short-read data were integrated using Unicycler v0.5 (https://github.com/rrwick/Unicycler) [25]. The resulting assemblies were polished with Pilon v1.24 (https://github.com/broadinstitute/pilon) [26] to obtain complete circular genomes. Assembly quality was assessed based on BUSCO completeness scores (>98%) (https://busco.ezlab.org) [27] and contig N50 values (>500 kb). Multilocus sequence typing (MLST) was carried out using mlst v2.23 (https://pubmlst.org/multilocus-sequence-typing) [28].

2.3. Construction of a global ST3014 E. coli database

A global ST3014 *E. coli* database was constructed by retrieving genomes from EnteroBase (accessed in June 2025, https://enterobase.warwick.ac.uk) [29] using the search criterion "Sequence Type = 3014". A total of 78 complete genomes were downloaded, representing isolates collected from 23 countries over the period 2000–2023. In addition, three isolates reported in the published literature were also included.

To assess the broader genomic background of ST3014, five representative continents (Asia, Europe, Oceania, North America, and South America) were selected based on the continental distribution of ST3014 isolates in EnteroBase.

For each continent, the country with the largest number of *E. coli* genomes available in NCBI was chosen (China, the United Kingdom, Australia, the United States, and Peru, respectively). From each country, 500 *E. coli* genomes were randomly sampled (2500 genomes in total) and subjected to MLST analysis. Only one additional ST3014 isolate was identified, originating from China and was included in the global ST3014 database.

Global distribution of ST3014 *E. coli* was visualized using the ChiPlot online platform (https://www.chiplot.online/) and BioRender (https://www.biorender.com).

Antimicrobial resistance genes (ARGs), and virulence factors (VFs), and plasmid replicons were identified using ABRicate v1.0 (https://github.com/tseemann/abricate) against the ResFinder [30], VFDB [31], and PlasmidFinder databases [32]. Circular barplots of ARGs and VFs were generated using Hiplot Pro (https://hiplot.com.cn/). To compare overall differences in ARG and VF profiles among isolates from different sources, Jaccard distances were calculated based on a binary presence/absence matrix. Principal coordinates analysis (PCoA) was performed using the vegan package in R v4.4.3, and results were visualized as two-dimensional scatterplots with 80% confidence ellipses. Differences between groups were assessed by permutational multivariate analysis of variance (PERMANOVA) with 9999 permutations. Differentially abundant ARGs among sources were identified using a LEfSe (Linear discriminant analysis Effect Size) workflow. Briefly, groupwise comparisons were first tested by the nonparametric Wilcoxon rank-sum test (R function wilcox.test) with Benjamini–Hochberg correction for multiple testing, and effect sizes were then estimated by linear discriminant analysis (LDA) using the lda function in the MASS package (https://cran.r-project.org/package=MASS); features with LDA score > 2.0 were considered significant. Final results are presented as barplots showing the effect sizes of differential features and their enrichment patterns across sources.

2.4. Phylogenetic and phylogeographic analyses

Core genes of all ST3014 *E. coli* isolates were identified by pan-genome analysis using Roary (https://github.com/sanger-pathogens/Roary) [33]. A maximum likelihood (ML) tree based on core genes alignment was constructed using FastTree (http://www.microbesonline.org/fasttree/) [34] to infer the evolutionary relationships among all ST3014 *E. coli* isolates. The tree was subsequently visualized using the ChiPlot online platform (https://www.chiplot.online/). Meanwhile, average nucleotide identity (ANI) analysis [35] (https://github.com/ParBLiSS/FastANI) was performed on all ST3014 genomes to assess genomic relatedness, and the results were visualized as a clustered heatmap.

To estimate the evolutionary timescale and infer the geographic origin of the ST3014 lineage, a relaxed molecular clock model implemented in treedater (https://github.com/emvolz/treedater) [36] was applied to the ML phylogeny to infer the time to the most recent common ancestor (tMRCA). Given the weak temporal signal ($R^2 \approx 0.04$) and high-rate heterogeneity (coefficient variation >1), parametric confidence intervals were not reported, and only point estimates were retained. Phylogeographic inference was conducted using a hierarchical strategy. First, sampling locations were aggregated at the continental level, and ancestral states across the entire phylogeny were reconstructed using the ace() function implemented in the ape package [35] under an equal-rates (ER) model. Subsequently, within continent-specific subtrees, ancestral states were reconstructed at the country level, and the ML estimates along with their probabilities were reported. To illustrate the transnational dissemination patterns of ST3014, the time-scaled phylogeny was integrated with geographic information to generate a global transmission map. All data processing, statistical analyses, and visualization were conducted in the R v4.4.3 using the ggplot2 (https://ggplot2.tidyverse.org), dplyr (https://dplyr.tidyverse.org), and sf packages (https://r-spatial.github.io/sf/). Country locations were defined using centroid coordinates corresponding to ISO3 country codes.

2.5. Plasmid database construction, visualization, and transferability prediction

A global plasmid database was constructed by searching for the Plasmids in Pathogens database (PIPdb) (https://nmdc.cn/pipdb/) [37] using the E44 bla_{NDM-5}-carrying plasmid as reference. For each alignment, query coverage (qcov), subject coverage (scov), and weighted identity (wid) were calculated. As the reference database mainly contains plasmid fragments, scov was generally low; therefore, filtering was based only on qcov and wid, retaining records with wid ≥90% and qcov ≥70%. This yielded a curated set of 152 homologous plasmid records from PIPdb, effectively removing low-relevance hits while minimizing the loss of homologous plasmids due to database fragmentation. After inclusion of E44-plasmid1, a total of 153 plasmids were used for phylogenetic analysis.

BLAST searches against the curated plasmid database identified 12 plasmids carrying bla_{NDM-5}. Transferability of the bla_{NDM-5}-carrying plasmids was predicted in silico using the MOB-typer module of MOB-suite v3.1.9 [38] (https://github.com/phac-nml/mob-suite) with

default parameters. Transferability classification was determined based on replicon type, relaxase type, mate-pair formation (MPF) system type, and origin of transfer (oriT). Host range predictions were also generated. The plasmids were visualized using the Proksee online platform (https://proksee.ca).

2.6. Analysis of bla_{NDM}-carrying gene clusters

The genetic environments surrounding bla_{NDM-5} in the 12 plasmids were visualized using gggenes package (https://wilkox.org/gggenes/) in R v4.4.3 with Coding sequence (CDS) regions extracted from GFF files and classified into functional categories (e.g., bla_{NDM}, insertion sequences, transposons, plasmid replicons). Using the respective bla_{NDM-5} loci as reference points, the relative start and end positions of neighboring genes were calculated, and ± 10 kb flanking regions were selected for visualization.

2.7. Phylogenetic analysis of plasmids

To investigate the phylogenetic relationships among all 153 plasmids (152 hits from PIPdb plus E44-plasmid1 = 153 total plasmids for phylogenetic analysis), we employed the MashTree (https://github.com/lskatz/mashtree) [39] software to construct a phylogenetic tree based on intergenomic Mash distances. Visualization was conducted on the ChiPlot online platform (https://www.chiplot.online/). Sample metadata, including plasmid type, source, collection year, as well as the distribution of ARGs and plasmid replicons, were mapped onto the tree for integrated interpretation.

3. Results

3.1. Identification of E. coli strains harboring bla_{NDM-5}

A total of 60 rectal swab samples were collected from piglets. From each sample, at least one colony was selected for further analysis, and in 12 cases two colonies were chosen, yielding a total of 72 isolates. Among the screened colonies, 44 isolates were confirmed as *E. coli*. After screening on meropenem (2 μg/mL)-containing medium, two suspected *Escherichia coli* isolates were recovered. PCR identification confirmed both isolates as *E. coli* (Fig. 1). Subsequent PCR screening further showed that both isolates carried the bla_{NDM} gene and were designated as strains E44 and E56.

Subsequent whole-genome sequencing showed that the two bla_{NDM}-positive isolates belonged to different sequence types and carried different bla_{NDM} variants: E44 was identified as bla_{NDM-5}-positive ST3014, whereas E56 was bla_{NDM-1}-positive ST9547. Because the main objective of this study was to resolve the genomic characteristics, global population structure, and plasmid background of a bla_{NDM-5}-positive ST3014 isolate, downstream lineage-focused analyses were centered on E44. E56 was retained as an additional bla_{NDM}-positive comparator identified during screening, but was not included in the ST3014-specific global analyses.

3.2. Global distribution and lineage context of the bla_{NDM-5}-positive ST3014 isolate E44

To characterize the global population structure of ST3014 and to ensure representativeness of the global ST3014 database, a total of 82 *E. coli* genomes were compiled, including one isolate (an environmental isolate from China) identified from a random screening of 2500 genomes in NCBI (500 each from Australia, China, Peru, the United Kingdom, and the United States). Among the 82 isolates, 56 had country metadata, and these isolates have been identified across five continents of Asia (n = 21), Europe (n = 26), Oceania (n = 2), North America (n = 4), and South America (n = 3). Of these 56 isolates with country information, 53 also had source metadata (20 human, 27 animal, 6 environmental). Overall, ST3014 isolates were identified in 23 countries, with China accounting for the largest proportion (12.20%, 10/82), followed by Thailand (7.32%, 6/82) and Switzerland (6.10%, 5/82) (Fig. 2).

3.3. The ARGs and VF profiles and phylogenetic relationships of ST3014 E. coli strains

E44 harbors six ARGs, including the metallo-β-lactamase gene bla_{NDM-5}, the aminoglycoside-modifying enzymes genes *aac*(3)-*IId* and *aadA2*; the efflux pump determinants genes *cmlA1* and *mdf*(A); and the trimethoprim resistance gene *dfrA12*. The ARG burden in E44 is lower than the ST3014 lineage average (≈11.84 ARGs). Among all ST3014 isolates, four strains were found to harbor the bla_{NDM} gene including two carrying bla_{NDM-1} and two carrying bla_{NDM-5}. In addition, *mdf*(A) (100%, 82/82), *tet*(A) (82.93%, 68/82), *sul2* (73.17%, 60/82), *floR* (67.07%, 55/82), bla_{TEM-1B} (65.85%, 54/82) were the most prevalent ARGs among all ST3014 isolates (Fig. 3a).

The 21 human source isolates carried an average of 11.90 resistance genes per isolate, the 27 animal source isolates 10.74, and the 6 environmental source isolates 15.00. PCoA revealed significant differences in the ARGs profiles among the three interfaces (p = 0.0116) (Fig. 3b). Subsequent pairwise comparisons demonstrated that the difference in

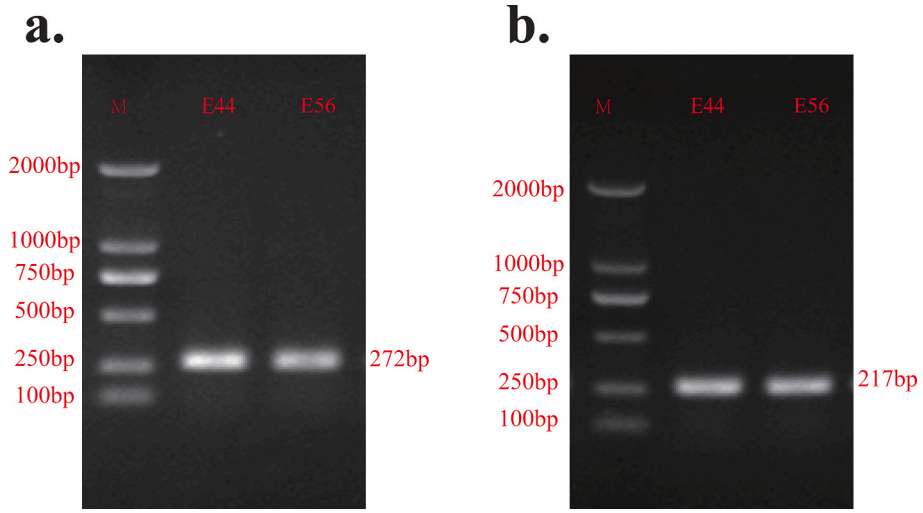

Fig. 1. PCR identification of *Escherichia coli* (a) and the bla_{NDM} gene (b). M: DNA marker. E44 and E56 refer to the codes assigned to the rectal swab samples.

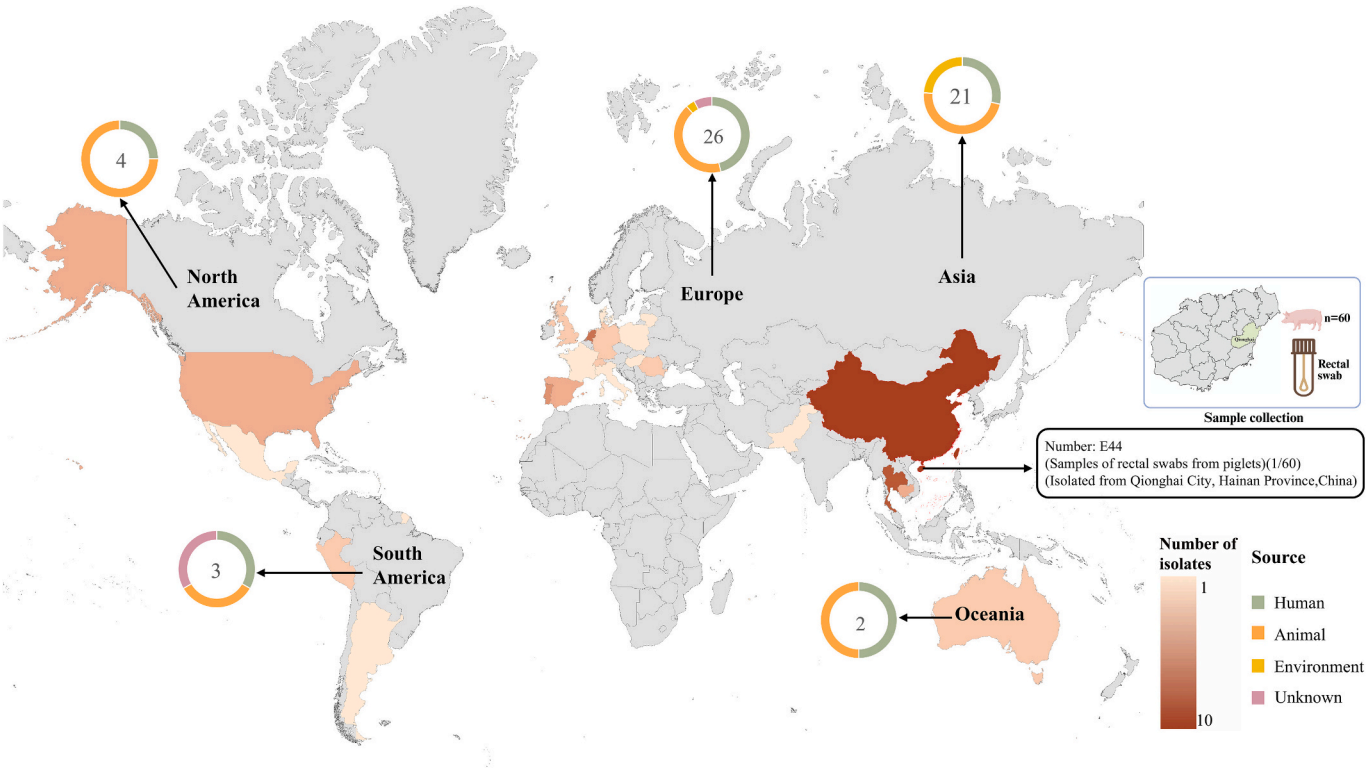

Fig. 2. Global distribution of ST3014 *Escherichia coli.*
The circular charts on each continent depict the composition of isolates by source (human, animal, and environment) (portion of figure created with BioRender.com).

ARGs profiles between the human and animal interfaces was statistically significant ($p = 0.0154$). Furthermore, LEfSe analysis indicated that the major differences were primarily driven by the ARGs *aadA2*, *dfrA12*, *mph*(A), *sul1*, *dfrA17*, and *aadA5*, which predominantly distinguished isolates from the human and animal interfaces (Fig. 3c).

E44 encodes 42 VFs spanning toxins, adhesins, iron acquisition systems, secretion systems, and outer membrane proteins, exceeding the ST3014 isolates average (≈37.12 VFs) (Fig. 3d). Among the four ST3014 isolates carrying the bla_{NDM} gene, the numbers of VFs were 37, 45, 41, and 46, respectively. The 21 human source isolates carried an average of 38.00 VFs per isolate, the 27 animal source isolates 36.93, and the 9 environmental source isolates 35.56. PCoA revealed that the differences in VF profiles among the three groups were not statistically significant ($p = 0.1017$) (Fig. 3e).

To evaluate overall genomic relatedness among ST3014 isolates, average nucleotide identity (ANI) analysis was performed. All isolates from different sources showed uniformly high ANI values (>99.54%) (Fig. 3f). In addition, a core gene-based phylogenetic tree was constructed for all ST3014 isolates (Fig. 3g). The E44 isolate clustered within the broader ST3014 population, with isolates from human, animal, and environmental sources interspersed throughout the phylogeny. E44 grouped with ESC_EA7466AA within clade 1, which comprised 13 strains, including three from human, four from animal, and two from environmental sources, source metadata were unavailable for the remaining 4 isolates. Of these 13 strains, six were isolated in Europe and two in Asia, whereas geographic metadata were unavailable for the remaining 5 isolates.

3.4. The global transmission of ST3014 E. coli

A time-scaled phylogeographic tree of the global ST3014 collection was reconstructed to infer the evolutionary timeline and geographic dispersal of this lineage (Fig. S2). The estimated time to the most recent common ancestor (tMRCA) was 1964.

Phylogeographic reconstruction suggested that ST3014 was most likely associated with an Asia origin (posterior probability = 0.262). At the country level, China showed the highest probability (0.383), exceeding those of other Asian countries.

To further visualize the inferred dissemination routes, the dated phylogeny was integrated with geographic information to generate a global transmission map (Fig. 4). Among all transmission pathways, China showed the highest number of inferred outgoing transmission links in the reconstructed dataset ($n = 16$), followed by the Netherlands ($n = 6$) and Thailand ($n = 4$). As for recipient countries, China also appeared as a recipient in several inferred transmission events (n = 4), followed by the United States, Spain, the Netherlands, Thailand, and Portugal, each occurring twice. Given the weak temporal signal, these phylogeographic patterns should be interpreted as exploratory rather than definitive. Within the reconstructed dataset, China showed the largest number of inferred outgoing links and also appeared as a recipient in several transitions. These patterns suggest that China may have acted as an important node in the sampled transmission network, although this inference remains exploratory given the weak temporal signal and sampling limitations. Notably, in the reconstructed dataset, the branch containing E44 was linked to an inferred China–Netherlands transition around 2016; however, this pattern should be interpreted cautiously given the weak temporal signal and sampling limitations. Furthermore, within the reconstructed dataset, China and the Netherlands were linked by multiple inferred transitions, with both countries appearing as source and recipient nodes.

3.5. Characteristics of the bla_{NDM-5} harboring plasmid

Four plasmids were identified in the E44 isolate, including one resistance plasmid designated E44-plasmid1 that carried the bla_{NDM-5} gene. Replicon typing classified E44-plasmid1 as an IncF-family plasmid. Bioinformatic prediction indicated that E44-plasmid1 carries mobility-associated elements consistent with predicted conjugative

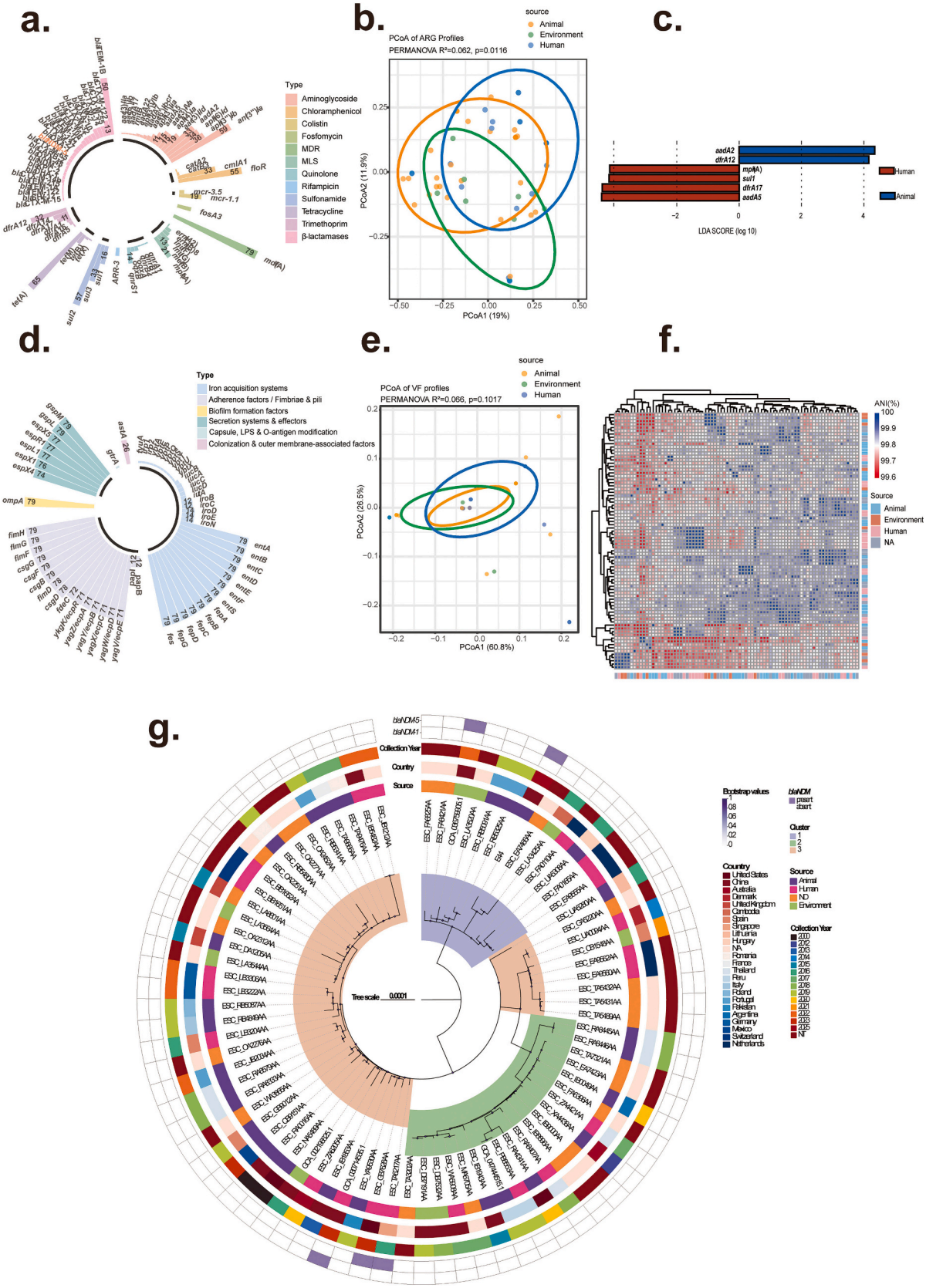

Fig. 3. Genomic characteristics of ST3014 *Escherichia coli*.

a. The ARG profiles of ST3014 isolates. Different colors represent distinct ARG categories, while bar height indicates the number of each ARG. b. PCoA plot of ARG repertoires across the three interfaces. c. LEfSe analysis of ARG repertoires between the human and animal interfaces. d. The VF profiles of ST3014 isolates. Different colors represent distinct VF categories, while bar height indicates the number of each VF. e. PCoA plot of VF profiles across the three interfaces. f. ANI analysis of all ST3014 isolates. g. Maximum-likelihood phylogenetic tree of ST3014 isolates constructed based on core genome sequences.

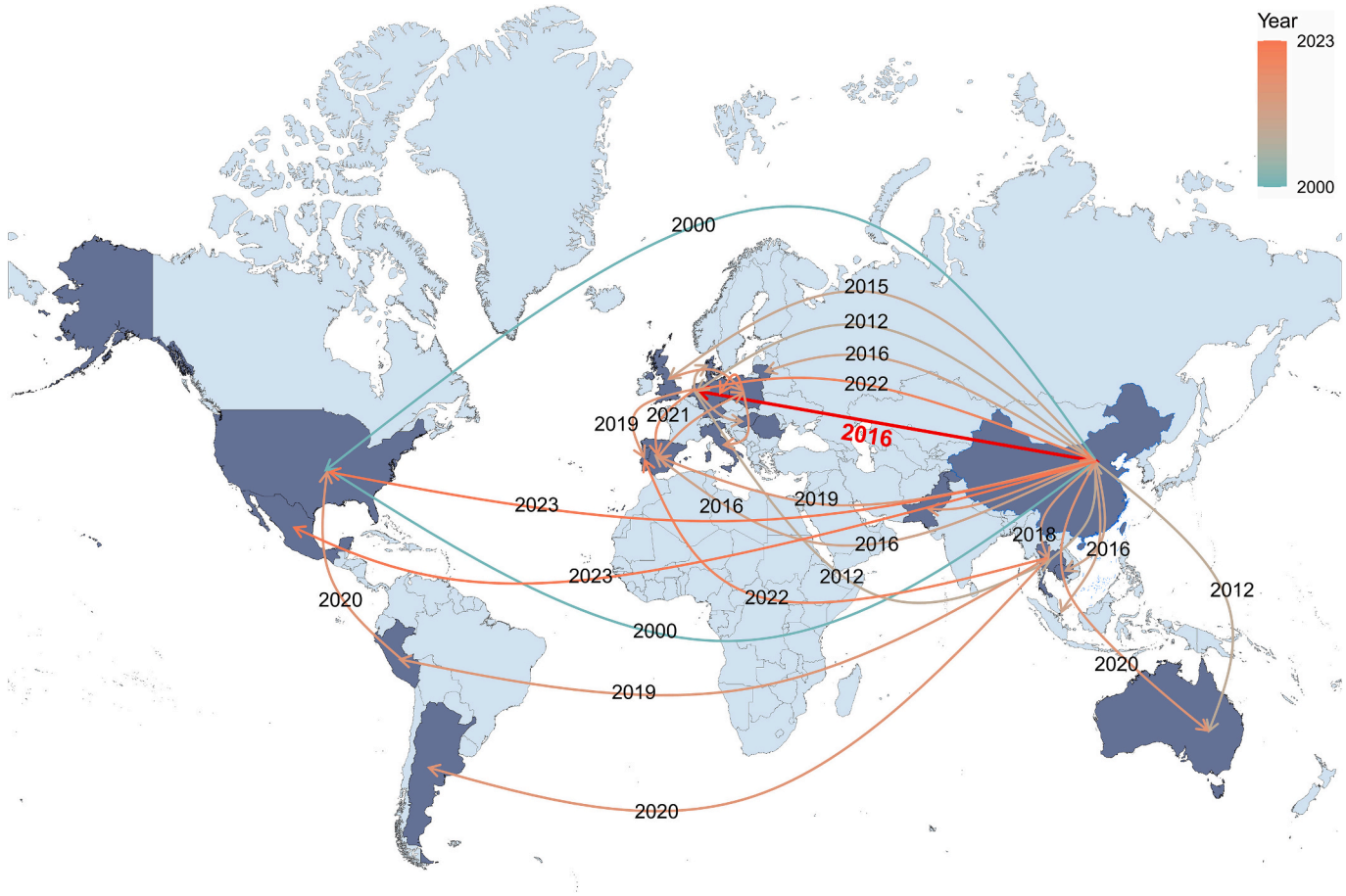

Fig. 4. Global transmission routes of ST3014 *E. coli* inferred from the dated phylogeographic reconstruction.
Arrows represent inferred international transmission events, with numbers indicating approximate years. Transmission pathways are shown as gradient-colored arrows ranging from light cyan (early) to orange-red (late), where darker colors indicate more recent events. The most recent transmission event involving the E44 isolate, between China and the Netherlands in 2016, is highlighted in bold red font.

potential, rather than experimentally confirmed transferability.

To examine the distribution of homologous plasmids, a search of the PIPDB database identified 152 homologous plasmid records showing related regions, with union coverage across the query region reaching 100%. After inclusion of E44-plasmid1, a total of 153 plasmids were considered in the subsequent phylogenetic analysis. These plasmids originated from multiple bacterial hosts, including *Escherichia coli*, *Salmonella enterica*, and *Klebsiella pneumoniae*. The most prevalent ARG was *sul1* (37.25%, 57/153), followed by *aadA5* (32.68%, 50/153) and *tet*(A) (28.76%, 44/153). In addition to other ARGs such as $bla_{\text{TEM-1}}$, $bla_{\text{CTX-M-14}}$, and *tet*(M), 12 plasmids carrying carbapenemase gene $bla_{\text{NDM-5}}$ were also detected.

Visualization of ±10 kb flanking regions surrounding $bla_{\text{NDM-5}}$ was performed for all 12 $bla_{\text{NDM-5}}$-carrying plasmids from the constructed plasmid database, including E44-plasmid1 (Fig. 5a). In E44-plasmid1, the downstream region was highly stable, with *ble*, *trpF*, and *dsbD* aligned in the same direction as a conserved module, whereas the upstream side showed greater variability, containing multiple insertion sequences such as *IS26* and other genes in mixed orientations. This structural pattern was also observed in most plasmids, which consistently carried the companion genes *ble*, *trpF*, and *dsbD*, forming a highly conserved modular structure. Among them, three plasmids lacked the *ble* gene but retained *trpF* and *dsbD*. *IS26* was the most frequently detected insertion sequence in the $bla_{\text{NDM-5}}$ flanking regions. Notably, *IS26* was repeatedly located adjacent to the variable upstream segment of the resistance cluster, whereas the downstream *ble-trpF-dsbD* segment remained relatively conserved. This configuration is consistent with *IS26*-mediated local recombination and restructuring around the $bla_{\text{NDM-5}}$ locus, suggesting that *IS26* likely contributed to capture, rearrangement, and diversification of the surrounding accessory region during plasmid evolution.

When the flanking structures were interpreted together with plasmid phylogenetic relatedness, $bla_{\text{NDM-5}}$ appeared to be embedded within a conserved mobile module that was maintained across related IncF-type plasmids but inserted into locally variable upstream contexts. This pattern suggests that dissemination of $bla_{\text{NDM-5}}$ in our dataset was driven not only by spread of related plasmid backbones, but also by modular remodeling of the $bla_{\text{NDM-5}}$ locus during plasmid evolution.

Further transferability prediction of all the 12 plasmids revealed that they were complete, single-contig plasmids, ranging in size from 120 to 212 kb, with GC contents of approximately 52%, consistent with that of Enterobacterales genomes. Replicon analysis showed that these plasmids commonly carried IncF family multi-replicon structures (e.g., IncFIA, IncFIB, IncFIC, IncFII).

With respect to mobility-associated elements, all plasmids carried a MOBF relaxase, while several plasmids additionally harbored a MOBP relaxase or MOBP-type oriT. All plasmids contained a MOBF-type oriT and generally carried MPF-associated elements consistent with predicted conjugative potential; some also encoded MPF_T or MPF_Unknown elements, indicating structurally complex mobility-associated architectures.

Host range prediction consistently indicated that these plasmids are primarily disseminated within Enterobacterales. Mash nearest-neighbor comparisons revealed high similarity to previously reported *E. coli*

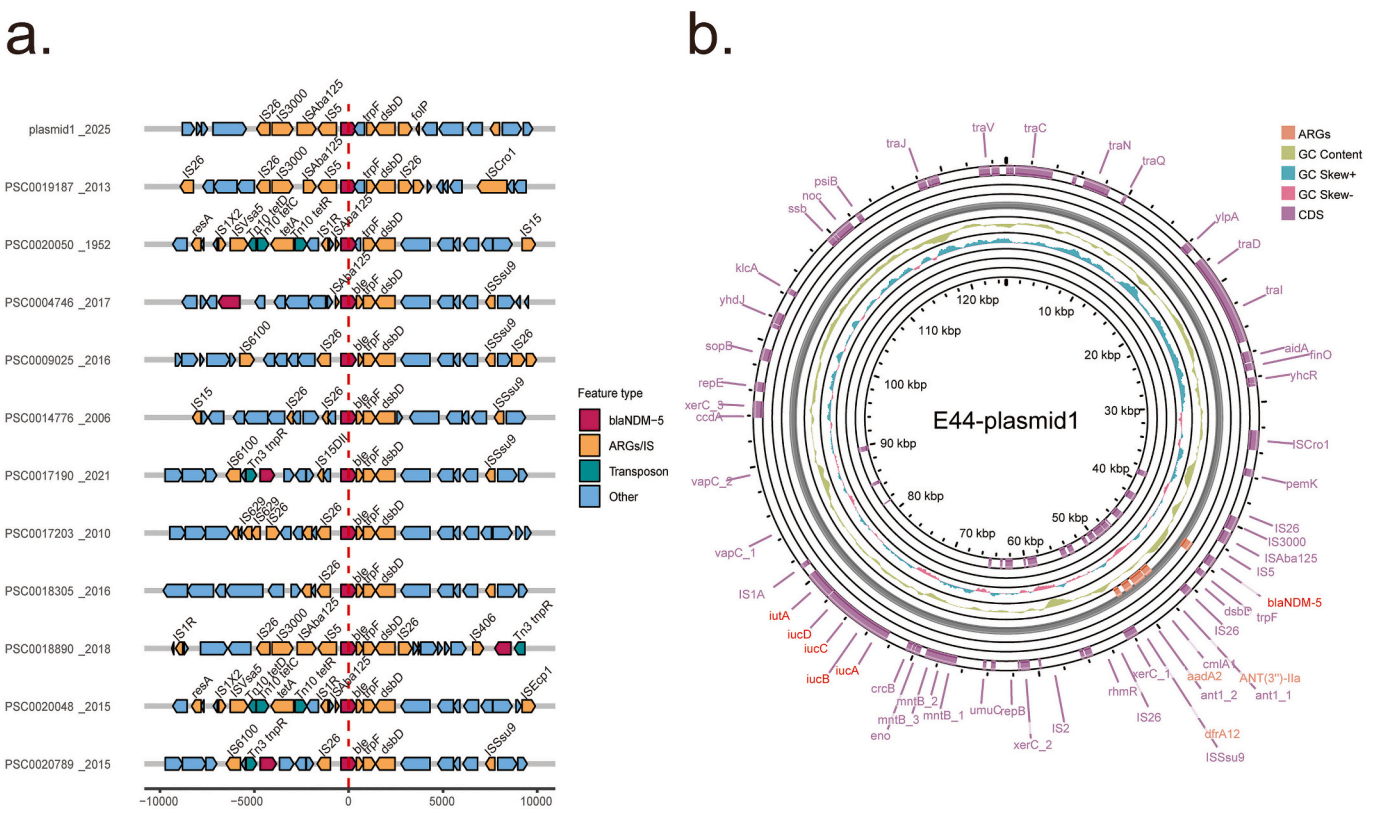

Fig. 5. Visualization of bla_{NDM-5}-associated gene clusters and the E44 bla_{NDM-5}-carrying plasmid.
a. Gene cluster visualization of bla_{NDM-5}-carrying contigs from the plasmid database. b. Gene cluster visualization of the bla_{NDM-5}-carrying plasmid (E44-plasmid1) identified in the E44 isolate.

plasmids.

To further characterize the genomic context of bla_{NDM-5}, we performed full-length visualization of the plasmid assembled from the Qionghai isolate (Fig. 5b). The plasmid (E44-plasmid1) is approximately 124 kb in length and carries multiple resistance determinants, including bla_{NDM-5}, *ant*(3″)-*Ia*, *aadA2*, *dfrA12*, and *cmlA1*, all located adjacent to typical integron structures. In addition, transposase genes such as *IS1* and *IS3* were identified, suggesting potential for recombination and dissemination.

Based on the in silico prediction that the bla_{NDM}-carrying plasmid harbored conjugation-related elements, we further performed virulence factor prediction and analysis on E44-plasmid1. The results revealed that this plasmid harbors a complete *sitABCD* iron/manganese transport system as well as the aerobactin system (*iucABCD* + *iutA*). These VFs are recognized as typical VFs of uropathogenic *E. coli* (UPEC) and sepsis-associated strains, and are considered hallmark virulence determinants of ExPEC.

3.6. Phylogenetic analysis of the 153 plasmids

All 153 plasmid sequences in the constructed plasmid database were subjected to phylogenetic analysis, including E44-plasmid1 (Fig. 6). Multiple distinct clades were revealed with the branching topology showing a certain degree of correspondence to the host species, geographic origin, and resistance gene profiles of the plasmids. Species annotation indicated that the majority of plasmids originated from members of the Enterobacteriaceae, particularly *E. coli*, *Klebsiella pneumoniae*, *Salmonella enterica*, and *Shigella flexneri*. Notably, plasmids from the United States accounted for the largest proportion (18.95%, 29/153), and most plasmids were isolated from *E. coli* (81.05%, 124/153). Most plasmids were collected after 2010 (56.86%, 87/153), and the closest relatives of E44-plasmid1 were also identified among *E. coli*-derived plasmids collected in the 2010s. These observations highlight the temporal clustering of plasmid dissemination and provide a foundation for subsequent analyses of ARGs.

In terms of ARGs distribution, most plasmids harbored multiple ARGs, with carbapenemase genes such as bla_{NDM} and their associated gene modules exhibiting remarkable conservation. Only 12 plasmids carried the bla_{NDM-5} gene (7.84%, 12/153). In contrast, a subset of plasmids lacked detectable ARGs, suggesting possible gene loss or recombination events during their evolutionary history. Regarding VFs distribution, only 11 plasmids were devoid of pathogenic VFs (7.19%, 11/153). Notably, among the 12 plasmids carrying bla_{NDM-5}, only 3 lacked VFs (25.00%, 3/12), indicating that ARGs and VFs may undergo partial co-transfer.

From a temporal and geographic perspective, the collection period of these plasmids spanned from the 1950s to the 2020s, encompassing isolates from Europe, Asia, Africa, the Americas, and Oceania. This broad distribution underscores the long-term persistence and ongoing global dissemination of such plasmids. Importantly, phylogenetic clustering revealed that certain resistance–virulence co-harboring plasmids (e.g., E44-plasmid1) grouped together with plasmids from different countries and hosts. Further analysis showed that E44-plasmid1 was most closely related to plasmid PSC0019187, which was isolated from *Escherichia coli* in 2013.

4. Discussion

The global spread of bla_{NDM} has become an important clinical and One Health concern because bla_{NDM} variants are frequently mobilized by plasmids and have been detected across human, animal, and environmental interfaces [12,40,41]. ST3014 of *E. coli* has been infrequently described in the literature, and its epidemiological and genomic characteristics—particularly when carrying bla_{NDM}—are not yet well

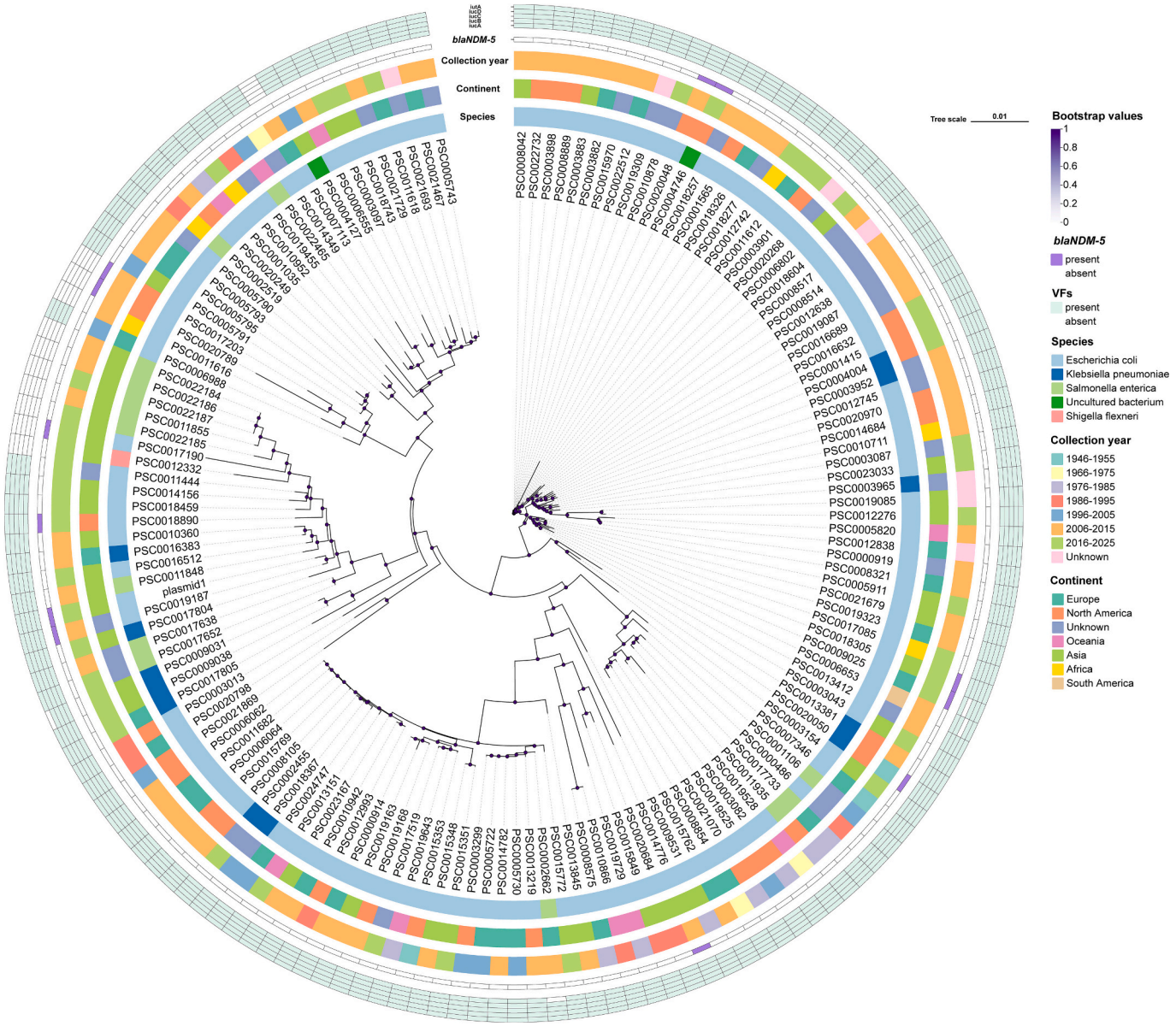

Fig. 6. Phylogenetic tree of plasmids with annotations of ARGs and replicons.

characterized. In this study we report a *bla*$_{\text{NDM-5}}$-bearing *E. coli* ST3014 isolate (E44) from piglets in tropical region of Hainan Province in China and, by compiling a global collection of ST3014 genomes and homologous plasmids, provide a systematic description of the clone's genomic features, plasmid architectures, and global phylogeography [20]. Among the two *bla*$_{\text{NDM}}$-positive isolates recovered in this screening, E44 was selected for in-depth analysis because it represented the *bla*$_{\text{NDM-5}}$-positive ST3014 lineage that formed the focus of our global lineage-level investigation, whereas E56 belonged to ST9547 and carried *bla*$_{\text{NDM-1}}$. These data improve understanding of a multi-interface ST lineage and emphasize that *bla*$_{\text{NDM}}$ warrant strengthened surveillance across clinical, agricultural and environmental settings.

Our phylogenetic and phylogeographic analyses place ST3014 within a lineage most likely originating in Asia, with China showing the highest country-level likelihood (posterior probability = 0.383) in our dataset. This inference was based on the time-scaled phylogeographic reconstruction of the global ST3014 dataset (Fig. S2), while Fig. 4 summarizes the inferred international transmission routes derived from the dated tree. The mid-20th century (1964) tMRCA estimate indicates long-standing diversification prior to recent international spread, implying that ST3014 has had sufficient time to acquire diverse accessory elements, including resistance plasmids. In the dated phylogeographic reconstruction, the branch containing E44 was linked to inferred cross-border movements involving China and the Netherlands, although these transitions should be interpreted cautiously given the weak temporal signal of the dataset. This finding indicates that ST3014 may have undergone repeated transnational dissemination since its mid-20th century origin, giving rise to a complex and dynamic global transmission network. ST3014 may share certain epidemiologically relevant features with ExPEC-associated lineages, but this study did not directly evaluate its phylogenetic relationship to ST131 clonal complexes [42]; this phylogenetic proximity may partly explain ST3014's capacity to capture clinically relevant plasmids such as those carrying *bla*$_{\text{NDM}}$ variants. Detection of ST3014 in a swine setting underscores the potential for agricultural environments with high animal density to act as amplification nodes for lineages that bridge animal, environment, and human reservoirs.

Across the compiled ST3014 collection, isolates from clinical, animal, and environmental sources commonly carry combinations of ARGs (including *bla*$_{\text{NDM}}$, *bla*$_{\text{OXA-1}}$, *aadA*, and *sul1*) and virulence loci (for

example fimH, *iucABCD–iutA*) [20,43]. This co-occurrence is epidemiologically relevant, as plasmids that co-harbor resistance and iron-uptake virulence systems can both promote survival under antimicrobial pressure and enhance extraintestinal fitness. IncF plasmid backbones that co-harbor siderophore systems (*iucABCD–iutA*) and carbapenemase genes [44] have been linked with ExPEC lineages and invasive clinical isolates [45]. The presence of such resistance–virulence plasmids in isolates sampled from different interfaces and from different years [13] suggests repeated plasmid acquisition or stable maintenance across niches rather than an isolated, single spillover event. For surveillance, this suggests that targeted screening should include agricultural, wastewater and clinical sampling to capture both lineage distribution and plasmid-associated dissemination signals over time.

IncF multi-replicon plasmids are known for their high plasticity, broad maintenance in Enterobacterales, and frequent carriage of both resistance and virulence determinants, and they are commonly implicated in the global dissemination of clinically important ARGs [44]. In our dataset, the $bla_{\text{NDM-5}}$ gene in E44 is located on an IncF multi-replicon plasmid that encodes a MOBF relaxase and a complete MPF_F system, a genetic configuration consistent with predicted conjugative potential within Enterobacterales [46]. Plasmid phylogeny and mash-based nearest-neighbor comparisons indicate close similarity between E44-plasmid1 and previously reported IncF plasmids from *E. coli* and other Enterobacterales, supporting the hypothesis that IncF backbones mediate cross-species spread of bla_{NDM} modules. Because IncF plasmids often carry multiple transfer and maintenance modules, they deserve prioritization in One Health plasmid surveillance.

E44-plasmid1 co-encodes $bla_{\text{NDM-5}}$ together with additional ARGs (e.g., *aadA2*, *ant* (3″)-*Ia*, *cmlA1*, and *dfrA12* in our assembly) and virulence-associated iron uptake systems (*sitABCD* and *iucABCD–iutA*). The coexistence of carbapenemase, aminoglycoside, and other ARGs on the same IncF plasmid backbone with predicted conjugative potential may amplify selective advantage under diverse antibiotic pressures, while siderophore systems may enhance colonization and extraintestinal survival [47]. Compared to homologous plasmids in our curated database, E44-plasmid1 shares the conserved bla_{NDM} module (*ble-trpF-dsbD*) and *IS26*-associated flanking architecture but may differ in accessory resistance gene composition and local insertion-sequence arrangement, indicating both conservation of a core mobilizable module and ongoing modular remodeling [13,48]. These shared and unique features together define E44-plasmid1 as a resistance–virulence co-harboring element with epidemiologically relevant differences from related plasmids.

Our comparative locus analyses confirm that bla_{NDM} variants are embedded within a conserved modular scaffold—commonly including *ble*, *trpF*, and *dsbD*—and flanked by insertion sequences such as *IS26* and *ISAba125* [11]. IS26 in particular appears recurrently adjacent to $bla_{\text{NDM-5}}$ modules and is well known to mediate the formation of composite transposons and translocatable units [50], promoting local rearrangements and gene capture. The conserved core (*ble-trpF-dsbD*) likely represents an evolutionarily conserved module that facilitates dissemination of the catalytic gene, while variation in surrounding *IS* elements and accessory genes reflects ongoing recombination events driven by selection and inter-plasmid exchange. Therefore, structural variants of *IS26*-associated bla_{NDM} modules represent practical molecular markers for tracking high-risk resistance cassettes in surveillance programs [13].

The phylogenetic topology we reconstructed shows multiple well-supported clades and intercontinental mixing, consistent with repeated international transmission events rather than a single point-source emergence [49]. The inferred tMRCA indicates a long evolutionary history, but short-branch diversification and low temporal signal limit our ability to precisely date recent spread; thus, inferred cross-border events should be interpreted cautiously. Geographic clustering of some clades suggests regional expansion followed by occasional long-distance dispersal, with plausible routes including livestock trade, food supply chains, and human travel [50]. Integrating denser temporal sampling, plasmid content mapping and recombination-aware phylogenetics will be necessary to resolve whether observed clade structure reflects clonal expansion, frequent plasmid exchange, or both.

There are several limitations of this study. First, ST assignment and global retrieval relied primarily on EnteroBase and public genomes, and we did not perform exhaustive ST screening across all available *E. coli* assemblies in other repositories; this may have missed additional ST3014 records and introduced sampling bias. Second, plasmid transferability and host range were inferred bioinformatically based on MOB-suite predictions and mobility-associated genetic signatures, but were not validated by conjugation assays. Therefore, the mobility of E44-plasmid1 should be interpreted as a predicted rather than experimentally confirmed characteristic. Third, although strain E44 was recovered under meropenem selection and was shown by genomic analysis to harbor $bla_{\text{NDM-5}}$, standardized antimicrobial susceptibility testing, including carbapenem MIC determination, was not performed in this study. As a result, the resistance phenotype of E44 could not be quantitatively assessed at the phenotypic level. Future work should incorporate conjugation assays and phenotypic AST testing to further validate plasmid transferability and resistance expression. Finally, plasmid phylogeny was reconstructed using mash distances that capture overall similarity but do not model plasmid recombination or segmental exchange, limiting our ability to identify precise plasmid origins, and given the weak temporal signal in our dataset, future inference of recent transmission should incorporate recombination-aware [50] and plasmid-aware [51] methods and denser sampling of suspected source populations to resolve short-term, cross-border movements.

From a One Health perspective, mitigating spread of ST3014-associated bla_{NDM} plasmids requires coordinated actions: stricter antimicrobial stewardship in livestock production [52], improved manure and wastewater treatment [53] to limit environmental dissemination of resistant bacteria and plasmids, strengthened farm biosecurity to reduce inter-interface exposure, and targeted genomic surveillance that integrates isolate sequencing from livestock, wastewater, and clinical sources. Prioritizing plasmid-level monitoring (tracking conserved bla_{NDM} modules and *IS26*-associated structural variants) will help detect and contain high-risk mobile elements before wider dissemination.

5. Conclusion

We characterized a $bla_{\text{NDM-5}}$–producing *E. coli* ST3014 isolate (E44) from piglets in tropical Hainan, resolving its complete genome and an IncF multi-replicon plasmid with predicted conjugative potential co-harboring resistance determinants ($bla_{\text{NDM-5}}$, *aadA2*, *ant* (3″) - *Ia*, *cmlA1*, *dfrA12*) and virulence-associated loci (*sitABCD*, *iucABCD–iutA*). Among the two bla_{NDM}-positive isolates identified in this study, E44 was selected for lineage-focused analysis because it was the only $bla_{\text{NDM-5}}$-positive ST3014 isolate. Integration of a global collection of ST3014 genomes ($n = 82$) and homologous plasmids ($n = 153$) suggested a likely Asian origin with China as the highest-likelihood source, frequent intermixing of human, animal, and environmental isolates, and a conserved bla_{NDM}-associated module (*ble-trpF-dsbD*) typically flanked by *IS26/ISAba125*. Plasmid analyses further showed that IncF multi-replicon backbones carried a MOBF relaxase and a complete MPF_F system, a genomic configuration consistent with predicted mobility within Enterobacterales. Together, these findings suggest that ST3014 may represent an underrecognized lineage of interest and that $bla_{\text{NDM-5}}$-carrying IncF plasmids may contribute to the dissemination of resistance and virulence traits. Our results underscore the importance of One Health-aligned surveillance that prioritizes plasmid-level monitoring, while also emphasizing the need for future functional validation of plasmid transferability, persistence, and control strategies.

CRediT authorship contribution statement

Zheng-Ze He: Conceptualization, Formal analysis, Methodology, Investigation, Software, Data curation, Writing—original draft

preparation, Visualization, Validation.

Chao Lv: Conceptualization, Formal analysis, Methodology, Software, Resources, Writing—review and editing, Visualization, Validation.

Feng Xie: Methodology, Investigation, Data curation, Validation.

Kun Wang: Methodology, Investigation.

Qing-Qing Zhang: Methodology, Investigation.

Wei-Ye Chen: Methodology, Writing—review and editing.

Ya-Qi He: Methodology, Data curation.

Yang Hong: Investigation.

Jing Xu: Conceptualization, Writing—review and editing, Supervision.

Xiao-Nong Zhou: Conceptualization, Resources, Writing—review and editing, Supervision, Funding acquisition, Project administration.

CRediT authorship contribution statement

Zheng-Ze He: Writing – original draft, Visualization, Validation, Software, Methodology, Investigation, Formal analysis, Data curation, Conceptualization. **Chao Lv:** Writing – review & editing, Visualization, Validation, Software, Resources, Methodology, Formal analysis, Conceptualization. **Feng Xie:** Validation, Methodology, Investigation, Data curation. **Kun Wang:** Methodology, Investigation. **Yang Hong:** Investigation. **Jing Xu:** Writing – review & editing, Supervision, Resources, Project administration, Funding acquisition, Conceptualization.

Informed consent statement

Not applicable.

Institutional review board statement

All experimental procedures involving animals were conducted in compliance with relevant ethical guidelines for animal research [54]. Authorization was obtained from the Ethics Review Committee of the National Institute of Parasitic Diseases, Chinese Center for Disease Control and Prevention (Chinese Center for Tropical Diseases Research) (Ref: IPD-2025-043).

Funding

This research was funded by the Key Research and Development Project of Hainan Province (No. ZDYF2024SHFZ083) and the Hainan Province Health Technology Innovation Joint Project (No. WSJK2024MS226).

Declaration of competing interest

The authors declare that they have no known competing financial interests or personal relationships that could have appeared to influence the work reported in this paper.

The authors declare that they have no known competing financial interests or personal relationships that could have appeared to influence the work reported in this paper.

Acknowledgments

We thank the team at Hainan Center for Tropical Diseases Research for their expertise and invaluable support with sampling and experiments. We thank Shanghai Tengyun Biotechnology Co., Ltd. for developing Hiplot Pro platform (https://hiplot.com.cn/) and providing technical assistance and valuable tools for data analysis and visualization.

Appendix A. Supplementary data

Supplementary data to this article can be found online at https://doi.org/10.1016/j.onehlt.2026.101409.

Data availability

The whole-genome shotgun project for Escherichia coli E44, including the plasmid sequence designated E44-plasmid1, has been deposited in DDBJ/ENA/GenBank under accession number JBWION000000000. The version described in this paper is JBWION010000000. The associated BioProject and BioSample accession numbers are PRJNA1441076 and SAMN56640175, respectively. All other data supporting the findings of this study are included in the article and its Supplementary Materials. Additional information is available from the corresponding author upon reasonable request.

References

[1] GBD 2021 Antimicrobial Resistance Collaborators, Global burden of bacterial antimicrobial resistance 1990–2021: a systematic analysis with forecasts to 2050, Lancet 404 (2024) 1199–1226, https://doi.org/10.1016/S0140-6736(24)01867-1.

[2] D. Nagarajan, N. Roy, O. Kulkarni, N. Nanajkar, A. Datey, S. Ravichandran, C. Thakur, T.S. Sandeep, I.V. Aprameya, S.P. Sarma, D. Chakravortty, N. Chandra, Ω76: a designed antimicrobial peptide to combat carbapenem- and tigecycline-resistant *Acinetobacter baumannii*, Sci. Adv. 5 (2019) eaax1946, https://doi.org/10.1126/sciadv.aax1946.

[3] W. Wu, Y. Feng, G. Tang, F. Qiao, A. McNally, Z. Zong, NDM metallo-β-lactamases and their bacterial producers in health care settings, Clin. Microbiol. Rev. 32 (2019) e00115-18, https://doi.org/10.1128/CMR.00115-18.

[4] R. Sharma, S. Patel, C. Abboud, J. Diep, N.S. Ly, J.M. Pogue, K.S. Kaye, J. Li, G. G. Rao, Polymyxin b in combination with meropenem against carbapenemase-producing *Klebsiella pneumoniae*: pharmacodynamics and morphological changes, Int. J. Antimicrob. Agents 49 (2017) 224–232, https://doi.org/10.1016/j.ijantimicag.2016.10.025.

[5] H. Sati, E. Carrara, A. Savoldi, P. Hansen, J. Garlasco, E. Campagnaro, S. Boccia, J. A. Castillo-Polo, E. Magrini, P. Garcia-Vello, E. Wool, V. Gigante, E. Duffy, A. Cassini, B. Huttner, P.R. Pardo, M. Naghavi, F. Mirzayev, M. Zignol, A. Cameron, E. Tacconelli, A. Aboderin, M. Al Ghoribi, J. Al-Salman, A. Amir, M. Apisarnthanarak, A. Blaser, El-Sharif, S. Essack, S. Harbarth, X. Huang, G. Kapoor, K. Knight, J.C. Muhwa, D.L. Monnet, T. Ousassa, R. Sacsaquispe, J. Severin, M. Sugai, N. Taneja, A. Umubyeyi Nyaruhirira, The WHO bacterial priority pathogens list 2024: a prioritisation study to guide research, development, and public health strategies against antimicrobial resistance, Lancet Infect. Dis. 25 (2025) 1033–1043, https://doi.org/10.1016/S1473-3099(25)00118-5.

[6] J. Huang, C. Lv, M. Li, T. Rahman, Y.-F. Chang, X. Guo, Z. Song, Y. Zhao, Q. Li, P. Ni, Y. Zhu, Carbapenem-resistant *Escherichia coli* exhibit diverse spatiotemporal epidemiological characteristics across the globe, Commun. Biol. 7 (2024) 51, https://doi.org/10.1038/s42003-023-05745-7.

[7] Y. Li, X. Sun, N. Dong, Z. Wang, R. Li, Global distribution and genomic characteristics of carbapenemase-producing *Escherichia coli* among humans, 2005–2023, Drug Resist. Updat. 72 (2024) 101031, https://doi.org/10.1016/j.drup.2023.101031.

[8] P. Nordmann, T. Naas, L. Poirel, Global spread of carbapenemase-producing Enterobacteriaceae, Emerg. Infect. Dis. 17 (2011) 1791–1798, https://doi.org/10.3201/eid1710.110655.

[9] W.X. Khong, E. Xia, K. Marimuthu, W. Xu, Y.-Y. Teo, E.L. Tan, S. Neo, P. U. Krishnan, B.S.P. Ang, D.C.B. Lye, A.L.P. Chow, R.T.-H. Ong, O.T. Ng, Local transmission and global dissemination of New Delhi metallo-β-lactamase (NDM): a whole-genome analysis, BMC Genomics 17 (2016) 452, https://doi.org/10.1186/s12864-016-2740-0.

[10] D. Yong, M.A. Toleman, C.G. Giske, H.S. Cho, K. Sundman, K. Lee, T.R. Walsh, Characterization of a new metallo-β-lactamase gene, blaNDM-1, and a novel erythromycin esterase gene carried on a unique genetic structure in *Klebsiella pneumoniae* sequence type 14 from India, Antimicrob. Agents Chemother. 53 (2009) 5046–5054, https://doi.org/10.1128/AAC.00774-09.

[11] S.R. Partridge, S.M. Kwong, N. Firth, S.O. Jensen, Mobile genetic elements associated with antimicrobial resistance, Clin. Microbiol. Rev. 31 (2018) e00088-17, https://doi.org/10.1128/CMR.00088-17.

[12] Y. Li, Y. Yang, Y. Wang, T.R. Walsh, S. Wang, C. Cai, Molecular characterization of blaNDM-harboring plasmids reveal its rapid adaptation and evolution in the Enterobacteriaceae, One Health Adv. 1 (2023) 30, https://doi.org/10.1186/s44280-023-00033-9.

[13] Q.-Y. Zhao, J.-H. Zhu, R.-M. Cai, X.-R. Zheng, L.-J. Zhang, M.-X. Chang, Y.-W. Lu, L.-X. Fang, J. Sun, H.-X. Jiang, IS26 is responsible for the evolution and transmission of blaNDM-harboring plasmids in *Escherichia coli* of poultry origin in China, mSystems 6 (2021) e00646-21, https://doi.org/10.1128/mSystems.00646-21.

[14] B.M. Marshall, S.B. Levy, Food animals and antimicrobials: impacts on human health, Clin. Microbiol. Rev. 24 (2011) 718–733, https://doi.org/10.1128/CMR.00002-11.
[15] S. Abraham, H.S. Wong, J. Turnidge, J.R. Johnson, D.J. Trott, Carbapenemase-producing bacteria in companion animals: a public health concern on the horizon, J. Antimicrob. Chemother. 69 (2014) 1155–1157, https://doi.org/10.1093/jac/dkt518.
[16] F.Y. Ramírez-Castillo, A.L. Guerrero-Barrera, F.J. Avelar-González, An overview of carbapenem-resistant organisms from food-producing animals, seafood, aquaculture, companion animals, and wildlife, Front. Vet. Sci. 10 (2023) 1158588, https://doi.org/10.3389/fvets.2023.1158588.
[17] B. Tang, J. Chang, L. Cao, Q. Luo, H. Xu, W. Lyu, M. Qian, X. Ji, Q. Zhang, X. Xia, H. Yang, Characterization of an NDM-5 carbapenemase-producing *Escherichia coli* ST156 isolate from a poultry farm in Zhejiang, China, BMC Microbiol. 19 (2019) 82, https://doi.org/10.1186/s12866-019-1454-2.
[18] L. Zhao, J. Zhang, B. Zheng, Z. Wei, P. Shen, S. Li, L. Li, Y. Xiao, Molecular epidemiology and genetic diversity of fluoroquinolone-resistant *Escherichia coli* isolates from patients with community-onset infections in 30 Chinese county hospitals, J. Clin. Microbiol. 53 (2015) 766–770, https://doi.org/10.1128/JCM.02594-14.
[19] B. Zheng, C. Huang, H. Xu, L. Guo, J. Zhang, X. Wang, X. Jiang, X. Yu, L. Jin, X. Li, Y. Feng, Y. Xiao, L. Li, Occurrence and genomic characterization of ESBL-producing, MCR-1-harboring *Escherichia coli* in farming soil, Front. Microbiol. 8 (2017) 2510, https://doi.org/10.3389/fmicb.2017.02510.
[20] Y.-Y. Liu, T. Li, H. Yue, C. Yue, L. Lu, J. Chen, H. Deng, X. Gao, J.-H. Liu, Occurrence and characterization of NDM-5-producing *Escherichia coli* from retail eggs, Front. Microbiol. 14 (2023) 1281838, https://doi.org/10.3389/fmicb.2023.1281838.
[21] S. Zhang, S. Chen, M.U. Rehman, H. Yang, Z. Yang, M. Wang, R. Jia, S. Chen, M. Liu, D. Zhu, X. Zhao, Y. Wu, Q. Yang, J. Huang, X. Ou, S. Mao, Q. Gao, D. Sun, B. Tian, A. Cheng, Distribution and association of antimicrobial resistance and virulence traits in *Escherichia coli* isolates from healthy waterfowls in Hainan, China, Ecotoxicol. Environ. Saf. 220 (2021) 112317, https://doi.org/10.1016/j.ecoenv.2021.112317.
[22] M.U. Rehman, H. Yang, S. Zhang, Y. Huang, R. Zhou, S. Gong, Q. Feng, S. Chen, J. Yang, Z. Yang, M. Abbas, M. Cui, M. Wang, R. Jia, S. Chen, M. Liu, D. Zhu, X. Zhao, Y. Wu, Q. Yang, J. Huang, L. Zhang, Y. Liu, Y. Yu, B. Tian, A. Cheng, Emergence of *Escherichia coli* isolates producing NDM-1 carbapenemase from waterfowls in Hainan island, China, Acta Trop. 207 (2020) 105485, https://doi.org/10.1016/j.actatropica.2020.105485.
[23] F.J. Zhao, G.B. Gu, J.C. Li, Z. Wang, Establishment and preliminary application of PCR for detecting *Escherichia coli* [in chinese], Prog. Vet. Med. 37 (8) (2016) 11–14, https://doi.org/10.16437/j.cnki.1007-5038.2016.08.003.
[24] Y. Chen, M. Li, B. Sun, L. Xia, Y. Zhang, J. Feng, M. Chen, Z. Cheng, C. Lv, W. Chen, J. Huang, Q. Li, Y. Zhang, J. Shang, Y. Cao, T. Wang, Y. Liu, M. Wang, B. Zhang, X. Guo, S. Huang, Y. Zhu, Companion animals as sources of hazardous critically important antimicrobial-resistant *Escherichia coli*: genomic surveillance in shanghai, J. Hazard. Mater. 491 (2025) 137852, https://doi.org/10.1016/j.jhazmat.2025.137852.
[25] R.R. Wick, L.M. Judd, C.L. Gorrie, K.E. Holt, Unicycler: resolving bacterial genome assemblies from short and long sequencing reads, PLoS Comput. Biol. 13 (2017) e1005595, https://doi.org/10.1371/journal.pcbi.1005595.
[26] B.J. Walker, T. Abeel, T. Shea, M. Priest, A. Abouelliel, S. Sakthikumar, C. A. Cuomo, Q. Zeng, J. Wortman, S.K. Young, A.M. Earl, Pilon: an integrated tool for comprehensive microbial variant detection and genome assembly improvement, PLoS One 9 (2014) e112963, https://doi.org/10.1371/journal.pone.0112963.
[27] M. Manni, M.R. Berkeley, M. Seppey, F.A. Simão, E.M. Zdobnov, BUSCO update: novel and streamlined workflows along with broader and deeper phylogenetic coverage for scoring of eukaryotic, prokaryotic, and viral genomes, Mol. Biol. Evol. 38 (2021) 4647–4654, https://doi.org/10.1093/molbev/msab199.
[28] K.A. Jolley, J.E. Bray, M.C.J. Maiden, Open-access bacterial population genomics: BIGSdb software, the PubMLST.org website and their applications, Wellcome Open Res. 3 (2018) 124, https://doi.org/10.12688/wellcomeopenres.14826.1.
[29] Z. Zhou, N.-F. Alikhan, K. Mohamed, Y. Fan, Agama study group, m. Achtman, The EnteroBase user's guide, with case studies on Salmonella transmissions, *Yersinia pestis* phylogeny, and *Escherichia* core genomic diversity, Genome Res. 30 (2020) 138–152, https://doi.org/10.1101/gr.251678.119.
[30] V. Bortolaia, R.S. Kaas, E. Ruppe, M.C. Roberts, S. Schwarz, V. Cattoir, A. Philippon, R.L. Allesoe, A.R. Rebelo, A.F. Florensa, L. Fagelhauer, T. Chakraborty, B. Neumann, G. Werner, J.K. Bender, K. Stingl, M. Nguyen, J. Coppens, B.B. Xavier, S. Malhotra-Kumar, H. Westh, M. Pinholt, M.F. Anjum, N. A. Duggett, I. Kempf, S. Nykäsenoja, S. Olkkola, K. Wieczorek, A. Amaro, L. Clemente, J. Mossong, S. Losch, C. Ragimbeau, O. Lund, F.M. Aarestrup, ResFinder 4.0 for predictions of phenotypes from genotypes, J. Antimicrob. Chemother. 75 (2020) 3491–3500, https://doi.org/10.1093/jac/dkaa345.
[31] B. Liu, D. Zheng, Q. Jin, L. Chen, J. Yang, VFDB, A comparative pathogenomic platform with an interactive web interface, Nucleic Acids Res. 47 (2019) (2019) D687–D692, https://doi.org/10.1093/nar/gky1080.
[32] A. Carattoli, E. Zankari, A. García-Fernández, M. Voldby Larsen, O. Lund, L. Villa, F. Møller Aarestrup, H. Hasman, *In silico* detection and typing of plasmids using PlasmidFinder and plasmid multilocus sequence typing, Antimicrob. Agents Chemother. 58 (2014) 3895–3903, https://doi.org/10.1128/AAC.02412-14.
[33] A.J. Page, C.A. Cummins, M. Hunt, V.K. Wong, S. Reuter, M.T.G. Holden, M. Fookes, D. Falush, J.A. Keane, J. Parkhill, Roary: rapid large-scale prokaryote pan genome analysis, Bioinformatics 31 (2015) 3691–3693, https://doi.org/10.1093/bioinformatics/btv421.
[34] M.N. Price, P.S. Dehal, A.P. Arkin, FastTree 2 – approximately maximum-likelihood trees for large alignments, PLoS One 5 (2010) e9490, https://doi.org/10.1371/journal.pone.0009490.
[35] C. Jain, L.M. Rodriguez-R, A.M. Phillippy, K.T. Konstantinidis, S. Aluru, High-throughput ANI analysis of 90K prokaryotic genomes reveals clear species boundaries, Nat. Commun. 9 (2018) 5114, https://doi.org/10.1038/s41467-018-07641-9.
[36] E.M. Volz, S.D.W. Frost, Scalable relaxed clock phylogenetic dating, Virus Evol. 3 (2017) vex025, https://doi.org/10.1093/ve/vex025.
[37] Q. Zhu, Q. Chen, S. Gao, Z. Li, H. Zhou, Z. Cui, G. Fan, X. Liu, X. Wu, J. Ma, B. Kan, S. Hu, L. Wu, X. Lu, PIPdb: a comprehensive plasmid sequence resource for tracking the horizontal transfer of pathogenic factors and antimicrobial resistance genes, Nucleic Acids Res. 53 (2025) D169–D178, https://doi.org/10.1093/nar/gkae952.
[38] J. Robertson, J.H.E. Nash, MOB-suite: software tools for clustering, reconstruction and typing of plasmids from draft assemblies, Microb. Genom. 4 (2018) e000206, https://doi.org/10.1099/mgen.0.000206.
[39] L. Katz, T. Griswold, S. Morrison, J. Caravas, S. Zhang, H. Bakker, X. Deng, H. Carleton, Mashtree: a rapid comparison of whole-genome sequence files, J. Open Source Softw. 4 (2019) 1762, https://doi.org/10.21105/joss.01762.
[40] Z. Ma, B. Wang, D. Zeng, H. Ding, Z. Zeng, Rapid dissemination of blaNDM-5 gene among carbapenem-resistant *Escherichia coli* isolates in a yellow-feather broiler farm via multiple plasmid replicon, Pathogens 13 (2024) 387, https://doi.org/10.3390/pathogens13050387.
[41] H.S. Mohamed, L. Galal, J. Hayer, J.A. Benavides, A.-L. Bañuls, C. Dupont, G. Conquet, C. Carrière, Y. Dumont, M.-N. Didelot, A.-L. Michon, H. Jean-Pierre, M. H. Aboubaker, S. Godreuil, Genomic epidemiology of carbapenemase-producing gram-negative bacteria at the human-animal-environment interface in Djibouti City, Djibouti, Sci. Total Environ. 905 (2023) 167160, https://doi.org/10.1016/j.scitotenv.2023.167160.
[42] M.-H. Nicolas-Chanoine, X. Bertrand, J.-Y. Madec, *Escherichia coli* ST131, an intriguing clonal group, Clin. Microbiol. Rev. 27 (2014) 543–574, https://doi.org/10.1128/CMR.00125-13.
[43] Y. Duan, H. Gao, L. Zheng, S. Liu, Y. Cao, S. Zhu, Z. Wu, H. Ren, D. Mao, Y. Luo, Antibiotic resistance and virulence of extraintestinal pathogenic *Escherichia coli* (ExPEC) vary according to molecular types, Front. Microbiol. 11 (2020) 598305, https://doi.org/10.3389/fmicb.2020.598305.
[44] L. Villa, A. García-Fernández, D. Fortini, A. Carattoli, Replicon sequence typing of IncF plasmids carrying virulence and resistance determinants, J. Antimicrob. Chemother. 65 (2010) 2518–2529, https://doi.org/10.1093/jac/dkq347.
[45] T.J. Johnson, L.K. Nolan, Pathogenomics of the virulence plasmids of *Escherichia coli*, Microbiol. Mol. Biol. Rev. 73 (2009) 750–774, https://doi.org/10.1128/MMBR.00015-09.
[46] M. Rozwandowicz, M.S.M. Brouwer, J. Fischer, J.A. Wagenaar, B. Gonzalez-Zorn, B. Guerra, D.J. Mevius, J. Hordijk, Plasmids carrying antimicrobial resistance genes in Enterobacteriaceae, J. Antimicrob. Chemother. 73 (2018) 1121–1137, https://doi.org/10.1093/jac/dkx488.
[47] B. Han, C. Feng, Y. Jiang, C. Ye, Y. Wei, J. Liu, Z. Zeng, Mobile genetic elements encoding antibiotic resistance genes and virulence genes in *Klebsiella pneumoniae*: important pathways for the acquisition of virulence and resistance, Front. Microbiol. 16 (2025) 1529157, https://doi.org/10.3389/fmicb.2025.1529157.
[48] C.J. Harmer, R.M. Hall, *IS26*-mediated formation of transposons carrying antibiotic resistance genes, mSphere 1 (2016) E00038-16, https://doi.org/10.1128/mSphere.00038-16.
[49] A.R. Manges, H.M. Geum, A. Guo, T.J. Edens, C.D. Fibke, J.D.D. Pitout, Global extraintestinal pathogenic *Escherichia coli* (ExPEC) lineages, Clin. Microbiol. Rev. 32 (2019) e00135-18, https://doi.org/10.1128/CMR.00135-18.
[50] X. Didelot, R. Bowden, D.J. Wilson, T.E.A. Peto, D.W. Crook, Transforming clinical microbiology with bacterial genome sequencing, Nat. Rev. Genet. 13 (2012) 601–612, https://doi.org/10.1038/nrg3226.
[51] P.N.A. Harris, A.M. Wailan, Beyond the core genome: tracking plasmids in outbreaks of multidrug-resistant bacteria, Clin. Infect. Dis. 72 (2021) 421–422, https://doi.org/10.1093/cid/ciaa052.
[52] R. Laxminarayan, D. Sridhar, M. Blaser, M. Wang, M. Woolhouse, Achieving global targets for antimicrobial resistance, Science 353 (2016) 874–875, https://doi.org/10.1126/science.aaf9286.
[53] E.G. Lou, M. Harb, A.L. Smith, L.B. Stadler, Livestock manure improved antibiotic resistance gene removal during co-treatment of domestic wastewater in an anaerobic membrane bioreactor, Environ. Sci. Water Res. Technol. 6 (2020) 2832–2842, https://doi.org/10.1039/D0EW00387E.
[54] Code of Practice for the Housing and Care of Animals Bred, Supplied or Used for Scientific Purposes, The Stationery Office, Norwich, 2014.